



Modeling tuberculosis dynamics with vaccination and treatment strategies

Olumuyiwa James Peter^{a,b,*}, Dipo Aldila^c, Tawakalt Abosede Ayoola^d,
Ghaniyyat Bolanle Balogun^e, Festus Abiodun Oguntolu^f

^a Department of Mathematical and Computer Sciences, University of Medical Sciences, Ondo City, Ondo State, Nigeria

^b Department of Epidemiology and Biostatistics, School of Public Health, University of Medical Sciences, Ondo City, Ondo State, Nigeria

^c Department of Mathematics, Faculty of Mathematics and Natural Sciences, Universitas Indonesia, Depok 16424, Indonesia

^d Department of Mathematical Sciences, Osun State University, Osogbo, Nigeria

^e Department of Computer Science, University of Ilorin, Kwara State, Nigeria

^f Department of Mathematics, Federal University of Technology, Minna, Niger State, Nigeria

ARTICLE INFO

Editor name: Joshua Kiddy Asamoah

Keywords:

Tuberculosis

Vaccination

Treatment

Mathematical model

Basic reproduction number

ABSTRACT

Tuberculosis (TB) remains a leading cause of morbidity and mortality worldwide, worsened by the emergence of drug-resistant strains. The implementation of vaccination and observed treatment still becomes the most popular intervention in many countries. This study develops a mathematical model to analyze TB dynamics by considering the impact of integrated intervention vaccination and treatment strategy, and also taking into account the possibility of treatment failure and drug-resistant. The model constructed by dividing the population into six compartments: susceptible S , vaccinated V , latent L , active TB (I), drug-resistant TB D_r , and recovered R . Through a mathematical analysis of the dynamical properties of the proposed model, we demonstrated that the disease-free equilibrium point is always locally asymptotically stable when the basic reproduction number is less than one and unstable when it exceeds one. Moreover, the endemic equilibrium point is shown to exist uniquely only when the basic reproduction number is greater than one, and once it exists, it is always locally stable. For better visualization of the stability properties, we perform continuation simulations to generate a bifurcation diagram of our model, utilizing various bifurcation parameters. The Partial Rank Correlation Coefficient (PRCC) approach is used to carry out sensitivity analyses to determine the most sensitive parameters to the disease control. Simulation results show that increased vaccination rates efficiently reduce the susceptible population to increase the vaccinated population, decreasing disease transmission and lowering the burden of active and drug-resistant tuberculosis. Recovery rates after second-line treatment have a substantial impact on the dynamics of drug-resistant tuberculosis. Higher recovery rates result in faster rises in the recovered population and improved disease control. The findings emphasize the need for integrated measures, such as vaccination campaigns and enhanced treatment procedures, to reduce tuberculosis incidence, minimize drug resistance, and improve public health outcomes. These findings lay the groundwork for enhancing tuberculosis control programs, especially in countries with limited resources.

* Corresponding author.

E-mail address: peterjames4real@gmail.com (O.J. Peter).

<https://doi.org/10.1016/j.sciaf.2025.e02647>

Received 7 January 2025; Received in revised form 12 March 2025; Accepted 13 March 2025

Available online 19 March 2025

2468-2276/© 2025 The Authors. Published by Elsevier B.V. This is an open access article under the CC BY-NC-ND license (<http://creativecommons.org/licenses/by-nc-nd/4.0/>).

Introduction

Tuberculosis (TB) is a contagious infection caused by the bacterium *Mycobacterium tuberculosis* [1]. It primarily affects the lungs, although other organs can be involved. According to the World Health Organization, TB is one of the top ten causes of death worldwide, leading to 1.4 million fatalities in 2019. Its persistence and resurgence in certain regions, despite the availability of effective treatment, underscore the intricate interplay of factors influencing its spread, including social determinants, co-infection with HIV, and the emergence of multidrug-resistant strains [2]. The burden of TB is not evenly distributed; it disproportionately affects socioeconomically disadvantaged populations, where it exacerbates cycles of poverty and ill-health. These statistics reveal not only the public health impact of TB but also its broader socioeconomic implications. Understanding the transmission dynamics of TB is essential for developing targeted interventions. The disease's complex life cycle, featuring latent and active stages, poses significant challenges for control and elimination efforts. In latent TB infection, individuals harbor the bacterium without showing symptoms, and they are not infectious. However, a subset of these individuals may progress to active TB disease, at which point they become symptomatic and capable of transmitting the infection to others. Factors such as immune suppression can precipitate this transition, which complicates the prediction of outbreak patterns and the impact of public health interventions. Despite the long-established use of the Bacillus Calmette-Guérin (BCG) vaccine in the Expanded Program on Immunization (EPI), it remains the sole approved vaccine against tuberculosis (TB) and is one of the most commonly administered vaccines globally [3]. However, its effectiveness in protecting against pulmonary TB is inconsistent, and the duration of its protection is not well-defined. Tuberculosis remains the deadliest single infectious agent worldwide, causing approximately 1.5 million deaths in 2014, with 91% of these being adults. Additionally, of the 9.6 million new cases reported that year, 37% went either undiagnosed or unreported [4,5]. This highlights the significant need for new preventive strategies, such as novel TB vaccines, especially for protecting adults against pulmonary TB which poses clinical management challenges and is a major contributor to ongoing transmission. The consensus is that developing new TB vaccines is crucial for achieving the World Health Organization's (WHO) End TB Strategy goals for 2035 and the goal of eliminating TB as a public health issue by 2050. Currently, with 15 vaccine candidates undergoing clinical trials, including one in each of phases IIb and III, the pipeline for TB vaccines looks more promising than ever before [6].

Mathematical models have become indispensable tools in epidemiology to understand the dynamics and control of infectious disease [7–11], allowing researchers and policymakers to simulate the spread of diseases and assess the potential impact of public health interventions [12]. For TB, modeling can help predict outbreak dynamics, understand the roles of different risk factors, and evaluate the cost-effectiveness of various control strategies [13]. Traditional models have provided insights into the basic mechanics of TB transmission but often fail to encapsulate the disease's full complexity. As such, there is a critical need for more refined models that incorporate the nuances of TB epidemiology, including latency, variable infectiousness, and population heterogeneity. [14] developed a mathematical model for tuberculosis that includes seasonality, identification, and treatment, the model's results were evaluated against field data and showed consistency. [15] used mathematical modeling to investigate the dynamics of tuberculosis transmission, including reinfection and optimal control. [16] investigated the relationship between COVID-19 and tuberculosis, whereas [17] used simulations to optimize TB control techniques. [18] investigated how awareness influences tuberculosis transmission. [19] investigated a patchy epidemic model for tuberculosis. [20] proposed a dynamic TB disease model that considered both hospitalized and non-hospitalized infected populations. [21] presented a model to measure the impact of treatment on tuberculosis (TB) and examined infectious persons. Ullah et al. (2020) investigated the stability of tuberculosis under partial treatment conditions. Intan et al. [22] used the SEIR framework to study TB transmission, taking into account the presence of a latent group and vaccination of vulnerable populations. Their data indicated that increased vaccination rates reduce tuberculosis transmission. Numerous studies have presented mathematical models to examine TB's global stability and the influence of heterogeneity on its transmission (Okuonghae 2013; Liu 2011). A mathematical model for tuberculosis to assess the impact of vaccination and reinfection was analyzed by the authors in [23], where they show the possible appearance of backward bifurcation from their simple model. A more complex model for assessing the novel M72/AS01_E vaccine is discussed by authors in [24]. The model involved various sources of infection, such as relapse, reinfection, and treatment failure. The combination between case detection and treatment in the tuberculosis model is discussed by the authors in [25]. The authors calibrated their model parameters using yearly incidence data. Recently, authors in [26] conducted a mathematical analysis on TB transmission from several countries, when the involved medical masks and case detection in their model. [27–41] provide more insights into tuberculosis dynamics.

Tuberculosis (TB) remains a major global health challenge, particularly due to the emergence of drug-resistant strains, which complicate disease control efforts. Although treatment and vaccine are important approaches to managing tuberculosis, their efficacy is frequently restricted by issues including imperfect vaccine quality and possible treatment failure, which last mentioned can lead to the emergence of drug-resistant tuberculosis. On the other hand, no mathematical models fully integrate these aspects into a single framework, despite the importance of these problems. Therefore, this paper presents a new compartmental model of TB transmission that builds upon classical susceptible–infected–recovered (SIR) frameworks while incorporating advancements in the understanding of TB pathology and treatment. Furthermore, our model also accommodate the fact that vaccination of TB not give a perfect efficacy against TB infection [42] and possibility of treatment failure which may lead to drug-resistant condition [43]. Our model divides the population into compartments according to disease status — susceptible, vaccinated, latently infected, infectious, drug-resistant, and recovered. These compartments are interconnected through a series of differential equations that describe the rates of transition between states, informed by current knowledge of the biological and behavioral processes governing TB spread. The paper is organized as follows: The formulation of the TB model and the model description is presented in Section “Model Formulation”, the dynamical analysis and some basic properties of the proposed model is presented in Section “Dynamical analysis”, sensitivity analysis of the model with Partial Rank Correlation Coefficient (PRCC) approach is presented in Section “Sensitivity Analysis”, and results and discussion is presented in Section “Results and Discussion”, while the conclusion of the study is presented in Section “Conclusion”.

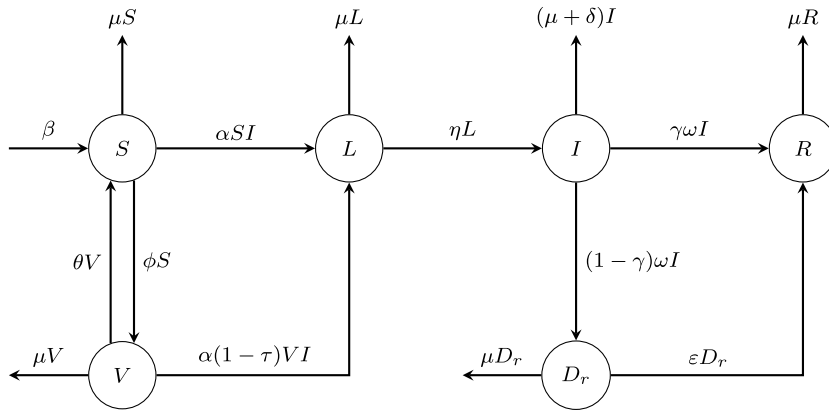


Fig. 1. Model's compartmental flow diagram.

Model formulation

We propose a novel mathematical model that describes the dynamics of tuberculosis (TB) transmission. The model divides the human population into six categories based on their health status: susceptible individuals $S(t)$, vaccinated individuals $V(t)$, individuals with latent tuberculosis $L(t)$, individuals with active tuberculosis $I(t)$, individuals with drug-resistant tuberculosis $D_r(t)$, and those who have recovered from tuberculosis $R(t)$. We assume that individuals in the latent population are infected with TB without exhibiting any symptoms. We define individuals in the drug resistance class as those who adopt the first-line treatment of TB (early treatment). The susceptible population is populated by immigration or newborns at a constant rate β and vaccine wane rate at the rate θ , also, the susceptible population is reduced by natural death and vaccine rate at the rate μ and ϕ respectively. We assume that TB infection can only be transmitted by active individuals. Thus, the force of infection is given by αSI , with α is the infection rate of TB. We also assume that, vaccinated population are partially protected due to the fact that vaccination is not 100% effective [44], after a period of time, the vaccinated individuals lose immunity. Thus, individuals vaccinated against TB can contract the disease through effective contact with those in the active TB class with a reduced rate $1 - \tau$ where τ represents the efficacy of the vaccine. We represent the force of infection for vaccinated individuals as $\alpha(1 - \tau)VI$. Latent individuals can progress to active TB class after incubation period of 2- 8 years after their initial infection [12,45]. We denote this transition rate from L to I compartment with parameter η . Individuals in the active TB class can recover at a rate ω with a proportion γ to recovered class through treatment and fraction of $1 - \gamma$ moves to drug resistance class as a results of improper or treatment failure [46]. Individuals in the active TB class can die as a result of TB infection at a rate δ while ε represents the recovery rate after second-line treatment. The equations in Eq. (1) represent the model description above, while the compartmental flow diagram of the model is shown in Fig. 1.

$$\begin{aligned}
 \frac{dS}{dt} &= \beta - \alpha SI + \theta V - (\mu + \phi)S, \\
 \frac{dV}{dt} &= \phi S - \alpha(1 - \tau)VI - (\mu + \theta)V, \\
 \frac{dL}{dt} &= \alpha SI + \alpha(1 - \tau)VI - (\mu + \eta)L, \\
 \frac{dI}{dt} &= \eta L - (\omega + \mu + \delta)I, \\
 \frac{dD_r}{dt} &= (1 - \gamma)\omega I - (\mu + \varepsilon)D_r, \\
 \frac{dR}{dt} &= \varepsilon D_r + \gamma\omega I - \mu R.
 \end{aligned}
 \tag{1}$$

Dynamical analysis

Taking the right-hand side of system (1) equal to zero, we have two types of equilibrium points of the respected model. The first equilibrium point is the TB-free equilibrium, denoted by \mathcal{E}_0 and is given by

$$\mathcal{E}_0 = (S^0, V^0, L^0, I^0, D_r^0, R^0) = \left(\frac{\beta(\mu + \theta)}{\mu(\mu + \phi + \theta)}, \frac{\beta\phi}{\mu(\mu + \phi + \theta)}, 0, 0, 0, 0 \right),
 \tag{2}$$

which represent an equilibrium when all non susceptible/vaccinated compartment equals to zero. Note that the total population at TB-free equilibrium is given by

$$N = S^0 + V^0 = \frac{\beta(\mu + \theta)}{\mu(\mu + \phi + \theta)} + \frac{\beta\phi}{\mu(\mu + \phi + \theta)} = \frac{\beta}{\mu}.$$

The second equilibrium point is the TB-endemic equilibrium point, denoted by \mathcal{E}_1 . This equilibrium represent a condition when the infected compartment also exist in the population. By direct calculation, we have \mathcal{E}_1 is given by:

$$\mathcal{E}_1 = (S, V, L, I, D_r, R) = (S^*, V^*, L^*, I^*, D_r^*, R^*), \tag{3}$$

where

$$S^* = \frac{\beta(\mu + \theta + \alpha I^*(1 - \tau))}{\alpha^2(1 - \tau)(I^*)^2 + \alpha(\theta + \phi(1 - \tau) + \mu(2 - \tau))}, \quad V^* = \frac{\beta\phi}{\alpha^2(1 - \tau)(I^*)^2 + \alpha(\theta + \phi(1 - \tau) + \mu(2 - \tau))},$$

$$L^* = \frac{\omega + \mu + \delta}{\eta} I^*, \quad D_r^* = \frac{(1 - \gamma)\omega}{\mu + \epsilon} I^*, \quad R^* = \frac{\omega(\mu\gamma + \epsilon)}{\mu(\mu + \epsilon)},$$

with I^* is taken from the positive roots of the following polynomial:

$$F(I) = a_2 I^2 + a_1 I + a_0 = 0, \tag{4}$$

and

$$a_2 = -\alpha^2(1 - \tau)(\mu + \eta)(\omega + \mu + \delta),$$

$$a_1 = \beta\eta(1 - \tau)\alpha^2 + (\mu\tau - 2\mu - \theta - \phi(1 - \tau))(\mu + \eta)(\delta + \mu + \omega)\alpha,$$

$$a_0 = \left(\frac{\alpha\beta(\phi(1 - \tau) + \mu + \theta)}{\mu(\mu + \phi + \theta)(\omega + \mu + \delta)(\mu + \eta)} - 1 \right) (\mu + \phi + \theta)(\mu + \eta)(\omega + \mu + \delta)\mu.$$

Calculation of the basic reproduction number

The basic reproduction number, \mathcal{R}_0 , is a pivotal parameter in epidemiology, often described as the average number of secondary cases produced by an infectious individual in a wholly susceptible population [47]. Our analysis not only derives this parameter but also examines its sensitivity to various factors, which can inform targeted control measures. We further explore the local and global stability of the model, utilizing Lyapunov functions to demonstrate the conditions under which the disease fades out or persists in the population. We use the Next-generation matrix approach introduced by authors in [48] to calculate the basic reproduction number of our model in (1). The transition and transmission matrix of sub-infected system of model in (1), denoted by V and F , respectively, is given by:

$$V = \begin{bmatrix} -\eta - \mu & 0 & 0 \\ \eta & -\omega - \mu - \delta & 0 \\ 0 & (1 - \gamma)\omega & -\mu - \epsilon \end{bmatrix}, \quad F = \begin{bmatrix} 0 & \frac{\beta(\mu + \theta)\alpha}{\mu(\mu + \phi + \theta)} + \frac{\alpha(1 - \tau)\beta\phi}{\mu(\mu + \phi + \theta)} & 0 \\ 0 & 0 & 0 \\ 0 & 0 & 0 \end{bmatrix}.$$

Since we have the second and the third row of F are zero, the recipes to calculate the next-generation matrix is given by

$NGM = -E^T F V^{-1} E$, with $E = \begin{bmatrix} 1 \\ 0 \\ 0 \end{bmatrix}$. By direct calculation, we have:

$$NGM = \left[\frac{\alpha\beta\eta(\phi(1 - \tau) + \mu + \theta)}{\mu(\mu + \phi + \theta)(\omega + \mu + \delta)(\mu + \eta)} \right]. \tag{5}$$

Hence, the basic reproduction number of system (1) is taken from the spectral radius of NGM , which is:

$$\mathcal{R}_0 = \frac{\alpha\beta\eta(\phi(1 - \tau) + \mu + \theta)}{\mu(\mu + \phi + \theta)(\omega + \mu + \delta)(\mu + \eta)}. \tag{6}$$

Several authors have utilized the basic reproduction number) to determine if a disease will persist or go into extinction in the population. The basic reproduction number is defined as the estimated number of secondary cases caused by a main case during one infectious period in a totally susceptible population. [49]. In most epidemiological models [50–53], it has been shown that a disease will persist in the population if the reproduction number is greater than one. Conversely, there is a possibility of disease elimination in the population if the basic reproduction number is less than one. For the proposed TB model in (1), we analyze the role of the reproduction number derived in (6) in the following subsection.

Existence of equilibrium points

Since the expression of the TB-free equilibrium point \mathcal{E}_0 is always exist in \mathbb{R}_6^+ without any condition related to the reproduction number, we have the following theorem.

Theorem 1. *The TB-free equilibrium of system (1) given by \mathcal{E}_0 in (2) always exist without any condition.*

Next, the TB-endemic equilibrium is given in Eq. (3), which could be positive or negative depends on the roots of polynomial $F(I) = 0$ in Eq. (4). If we have at least one positive roots, then we will have exactly one positive TB-endemic equilibrium. Hence, we need to adjust the possible existence of a positive roots that satisfies $F(I) = 0$. From the expression of \mathcal{R}_0 , we can see that a_0 of $F(I)$ can be rewritten as:

$$a_0 = (\mathcal{R}_0 - 1)(\mu + \phi + \theta)(\mu + \eta)(\omega + \mu + \delta)\mu.$$

Hence, since a_0 is always negative and $a_0 > 0 \Leftrightarrow \mathcal{R}_0 > 1$, then we will always have a multiplication of the root of $F(I)$ is always negative, which indicates a unique positive root. Hence, there is always exist a unique TB-endemic equilibrium if $\mathcal{R}_0 > 1$.

Next, we analyze the possibility of the existence of positive roots of $F(I)$ in the case of $\mathcal{R}_0 < 1$. We use a similar gradient method approach as the authors in [51]. The idea of this gradient method is to analyze the direction of $\frac{\partial I}{\partial \mathcal{R}_0}$ at the branching point $\mathcal{R}_0 = 1, I = 0$. If the gradient is positive, then there will be no endemic equilibrium point for any $\mathcal{R}_0 < 1$. On the other hand, if we can prove that the gradient could be negative in this branching point, then there will be an endemic equilibrium in the case of $\mathcal{R}_0 < 1$.

To analyze this possibility, let \mathcal{R}_0 as the bifurcation parameter. Hence, we need to rewrite $F(I)$ as a function of \mathcal{R}_0 . To do this, let we solve $\mathcal{R}_0 = 1$ respect to α , and substitute it to $F(I)$. By direct calculation, α that satisfies $\mathcal{R}_0 = 1$ is given by:

$$\alpha^* = \frac{\mu(\mu + \phi + \theta)(\omega + \mu + \delta)(\mu + \eta)}{\beta(\mu + \phi(1 - \tau) + \theta)\eta}$$

Substitute α^* into $F(I)$, and calculate $dfrac{\partial I}{\partial \mathcal{R}_0}$ at $I = 0$ gives

$$A_1 \frac{\partial I}{\partial \mathcal{R}_0} + (\mu + \phi + \theta)(\mu + \eta)(\omega + \mu + \delta)\mu = 0,$$

where

$$A_1 = -\frac{\mu(\mu + \phi + \theta)(\omega + \mu + \delta)^2(\mu + \eta)^2 [(\tau - 1)^2 \phi^2 + (1 - \tau)(2(\mu + \theta) - \mu\tau)\phi + (\mu + \theta)^2]}{\beta(-\phi\tau + \mu + \phi + \theta)^2 \eta}$$

Hence, we have

$$\frac{\partial I}{\partial \mathcal{R}_0}(\mathcal{R}_0 = 1, I = 0) = -\frac{(\mu + \phi + \theta)(\mu + \eta)(\omega + \mu + \delta)\mu}{A_1}$$

Since $2(\mu + \theta) - \mu\tau > 2\theta + \mu(1 - \tau) > 0$, then we have that A_1 is always negative. Hence, we have that $\frac{\partial I}{\partial \mathcal{R}_0}(\mathcal{R}_0 = 1, I = 0)$ is always non-negative.

With these result, we have the following Theorem

Theorem 2. TB model in (1) always has a unique endemic equilibrium if $\mathcal{R}_0 > 1$, and no TB-endemic equilibrium otherwise.

Stability analysis of the equilibrium points

Linearization technique will be used to analyze the local stability of TB-free equilibrium around \mathcal{R}_0 . By direct calculation, the Jacobian matrix of system (1) around \mathcal{E}_0 is given by:

$$J(\mathcal{E}_0) = \begin{bmatrix} -\phi - \mu & \theta & 0 & -\frac{\beta(\mu + \theta)\alpha}{\mu(\mu + \phi + \theta)} & 0 & 0 \\ \phi & -\mu - \theta & 0 & -\frac{\alpha(1 - \tau)\beta\phi}{\mu(\mu + \phi + \theta)} & 0 & 0 \\ 0 & 0 & -\eta - \mu & \frac{\beta(\mu + \theta)\alpha}{\mu(\mu + \phi + \theta)} + \frac{\alpha(1 - \tau)\beta\phi}{\mu(\mu + \phi + \theta)} & 0 & 0 \\ 0 & 0 & \eta & -\omega - \mu - \delta & 0 & 0 \\ 0 & 0 & 0 & (1 - \gamma)\omega & -\mu - \epsilon & 0 \\ 0 & 0 & 0 & \gamma\omega & \epsilon & -\mu \end{bmatrix} \tag{7}$$

There are four explicit eigenvalues of $J(\mathcal{E}_0)$, i.e.

$$\lambda_1 = -\mu, \lambda_2 = -\mu, \lambda_3 = -(\mu + \epsilon), \lambda_4 = -(\mu + \phi + \theta).$$

the other two eigenvalues are taken from the root of the following polynomial:

$$G(\lambda) = b_2\lambda^2 + b_1\lambda + b_0 = 0,$$

where

$$b_2 = \mu(\mu + \phi + \theta),$$

$$b_1 = (\mu + \phi + \theta)(\delta + \eta + 2\mu + \omega)\mu,$$

$$b_0 = (1 - \mathcal{R}_0)(\mu + \phi + \theta)(\mu + \eta)(\omega + \mu + \delta)\mu.$$

Since b_2 and b_1 are always positive, and $b_0 > 0 \Leftrightarrow \mathcal{R}_0 < 1$, then we will have the roots of $G(\lambda) = 0$ will always have a negative real part. This result was summarized in the following theorem.

Theorem 3. The TB-free equilibrium \mathcal{E}_0 of the TB model in system (1) is always locally asymptotically stable if $\mathcal{R}_0 < 1$ and unstable if $\mathcal{R}_0 > 1$.

For the stability of the endemic equilibrium, we use a center-manifold approach as mentioned in Castillo Chaves and Song bifurcation theorem [54]. The result is given in the following theorem.

Theorem 4. The Tuberculosis model in (1) always undergoes a forward bifurcation at $\mathcal{R}_0 = 1$.

Proof. Using the center manifold theory introduced by Castillo-Chavez and Song [54], we assume the following:

$$S = x_1, \quad V = x_2, \quad L = x_3, \quad I = x_4, \quad D_r = x_5, \quad R = x_6.$$

As a result, the system (1) can be reformulated as:

$$\begin{aligned} f_1 &= x_1' = \beta - \alpha x_1 x_4 + \theta x_2 - (\mu + \phi) x_1, \\ f_2 &= x_2' = \phi x_1 - \alpha (1 - \tau) x_2 x_4 - (\mu + \theta) x_2, \\ f_3 &= x_3' = \alpha x_1 x_4 + \alpha (1 - \tau) x_2 x_4 - (\mu + \eta) x_3, \\ f_4 &= x_4' = \eta x_3 - (\omega + \mu + \delta) x_4, \\ f_5 &= x_5' = (1 - \gamma) \omega x_4 - (\mu + \epsilon) x_5, \\ f_6 &= x_6' = \gamma \omega x_4 + \epsilon x_5 - \mu x_6. \end{aligned} \tag{8}$$

We choose α as the bifurcation parameter. When $\mathcal{R}_0 = 1$, solving Eq. (6) yields:

$$\alpha^* = \frac{\mu(\mu + \phi + \theta)(\omega + \mu + \delta)(\mu + \eta)}{\beta(-\phi\tau + \mu + \phi + \theta)\eta}$$

To proceed with the analysis, the Jacobian matrix of system (8) is evaluated at the disease-free equilibrium \mathcal{E}_0 with $\alpha = \alpha^*$, resulting in the following:

$$J = \begin{bmatrix} -\mu - \phi & \theta & 0 & -\frac{(\omega + \mu + \delta)(\mu + \eta)(\mu + \theta)}{(-\phi\tau + \mu + \phi + \theta)\eta} & 0 & 0 \\ \phi & -\mu - \theta & 0 & -\frac{(\omega + \mu + \delta)(\mu + \eta)(1 - \tau)\phi}{(-\phi\tau + \mu + \phi + \theta)\eta} & 0 & 0 \\ 0 & 0 & -\mu - \eta & \frac{(\omega + \mu + \delta)(\mu + \eta)(\mu + \theta)}{(-\phi\tau + \mu + \phi + \theta)\eta} + \frac{(\omega + \mu + \delta)(\mu + \eta)(1 - \tau)\phi}{(-\phi\tau + \mu + \phi + \theta)\eta} & 0 & 0 \\ 0 & 0 & \eta & -\omega - \mu - \delta & 0 & 0 \\ 0 & 0 & 0 & (1 - \gamma)\omega & -\mu - \epsilon & 0 \\ 0 & 0 & 0 & \gamma\omega & \epsilon & -\mu \end{bmatrix}.$$

The eigenvalue calculation for J reveals one simple zero eigenvalue, while the remaining five eigenvalues have negative. To identify the corresponding right eigenvector $w = (w_1, w_2, w_3, w_4, w_5, w_6)^T$ associated with the zero eigenvalue, we solve the equation $Jw = 0$, yielding the following expressions:

$$\begin{aligned} w_1 &= -(\mu + \eta) ((\mu + \theta)^2 + \phi\theta(1 - \tau)) (\omega + \mu + \delta) (\mu + \epsilon), \\ w_2 &= -(\mu + \epsilon) (\mu(2 - \tau) + \phi(1 - \tau) + \theta) (\mu + \eta) \phi (\omega + \mu + \delta), \\ w_3 &= (\omega + \mu + \delta) \mu (\mu + \epsilon) (\mu + \phi + \theta) (\phi(1 - \tau) + \mu + \theta), \\ w_4 &= \mu (\mu + \epsilon) (\mu + \phi + \theta) (\phi(1 - \tau) + \mu + \theta) \eta, \\ w_5 &= \omega (1 - \gamma) \mu (\mu + \phi + \theta) (\phi(1 - \tau) + \mu + \theta) \eta, \\ w_6 &= \omega (\gamma\mu + \epsilon) (\mu + \phi + \theta) (\phi(1 - \tau) + \mu + \theta) \eta. \end{aligned}$$

Similarly, let $v = (v_1, v_2, v_3, v_4, v_5, v_6)^T$ represent the left eigenvector corresponding to the zero eigenvalue. Solving $vJ = 0$ produces the following results:

$$v_1 = 0, \quad v_2 = 0, \quad v_3 = \eta, \quad v_4 = \mu + \eta, \quad v_5 = 0, \quad v_6 = 0$$

Since $v_1, v_2, v_5,$ and v_6 are all zero, it is not necessary to compute the derivatives of $f_1, f_2, f_5,$ and f_6 . However, for f_3 and f_4 , the relevant nonzero second derivatives are as follows:

$$\frac{\partial^2 f_3}{\partial x_1 \partial x_4} = \alpha^*, \quad \frac{\partial^2 f_3}{\partial x_2 \partial x_4} = \alpha^*(1 - \tau), \quad \frac{\partial^2 f_3}{\partial x_4 \partial \alpha^*} = \frac{\beta(\phi(1 - \tau) + \mu + \theta)}{\mu(\mu + \phi + \theta)}.$$

The bifurcation coefficients a and b , which determine the direction of bifurcation depending on their signs, are calculated as follows:

$$\begin{aligned} a &= \sum_{k,i,j=1}^n v_k w_i w_j \frac{\partial^2 f_k}{\partial x_i \partial x_j} (0, 0) \\ &= -\frac{2\eta}{\beta} \mu^2 (\mu + \eta)^2 (\omega + \mu + \delta)^2 (\mu + \epsilon)^2 (\mu + \phi + \theta)^2 \dots \\ &\times ((\mu + \theta)^2 + \phi\theta(1 - \tau) + (\mu(2 - \tau) + \phi(1 - \tau) + \theta) \phi(1 - \tau)) < 0 \\ b &= \sum_{k,i,j=1}^n v_k w_i \frac{\partial^2 f_k}{\partial x_i \partial \phi} (0, 0) \\ &= \beta \eta^2 (\phi(1 - \tau) + \mu + \theta)^2 (\mu + \epsilon) > 0. \end{aligned}$$

Since a is negative and b is positive, the system exhibits a forward bifurcation. \square

A consequences of Theorem 4 is that the endemic equilibrium \mathcal{E}_1 is locally asymptotically stable for $\mathcal{R}_0 > 1$ but close to one. A dynamical behavior for any \mathcal{R}_0 greater and far beyond one will be discussed numerically in the proceeding section.

Table 1
Model variables and their initial conditions.

Variable	Description	ICs	Value
$S(t)$	Susceptible humans	$S(0)$	10,000
$V(t)$	Vaccinated humans	$V(0)$	3000
$L(t)$	Latent humans	$L(0)$	8300
$I(t)$	Active TB humans	$I(0)$	8010
$D_r(t)$	Drug resistance humans	$D_r(0)$	0
$R(t)$	Recovered humans	$R(0)$	0

Table 2
Model parameter values and their interpretation with estimated values.

Parameter	Description	Value	Source
α	Transmission rate	1.57×10^{-8} per year	[55]
β	Recruitment rate	5	[56]
ϕ	Vaccination rate	0.1–0.98	[57]
θ	loss of immunity	0.10 per year	[58]
μ	Natural death rate	0.0142 per year	[59]
η	Progression rate from latent to active TB	0.129 per year	[12]
δ	TB induced death rate	0.1	[38]
ω	Movement rate out of active TB class	0.287 per year	[58]
ϵ	Rate of recovery after second line treatment	0.287 per year	[58]
τ	Vaccine efficacy	0–1	[60]
γ	Recovery rate of active TB individuals due to prompt treatment	0.129 per year	[12]
δ	Death rate due to TB	0.1 per year	[38]

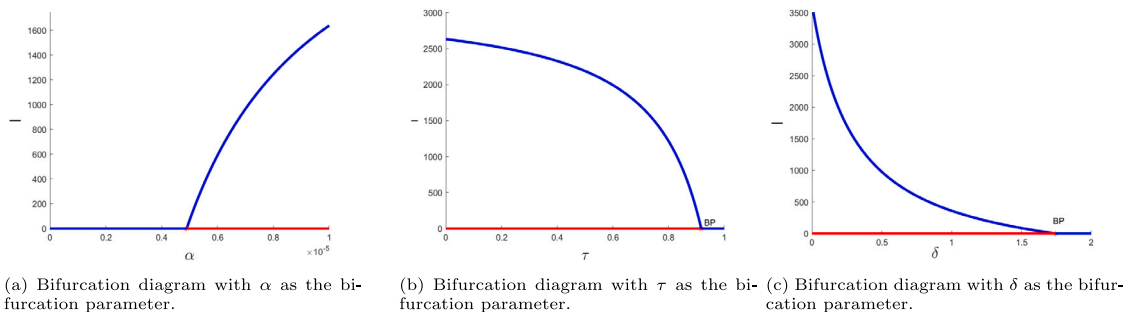


Fig. 2. Bifurcation diagram of model (1) with α , τ , and δ as the bifurcation parameter represented in panel a, b and c, respectively. The branching point appears at $\mathcal{R}_0 = 1$. The red and blue curve represent the unstable and stable equilibrium points, respectively. (For interpretation of the references to color in this figure legend, the reader is referred to the web version of this article.)

Bifurcation diagram

Here in this section we simulate our analytical results in the previous section using a bifurcation diagram. We use a parameter values as shown in Table 2, and conduct the numerical simulation using *MATCONT* which is based on MatLab. The first bifurcation diagram is shown in Fig. 2(a) where α becomes the bifurcation parameter. For a small α less than 4.89×10^{-6} , we have a stable disease-free equilibrium, which is denoted by the solid blue curve. The stability of disease-free equilibrium maintain until it meets the Branching Point (BP) at $\alpha = 4.89 \times 10^{-6}$. Meeting BP, the stability of disease-free equilibrium changes into unstable equilibrium. In the same time, the endemic equilibrium start to arise and keep increasing as α increases.

The second bifurcation diagram is shown in Fig. 2(b) where we choose τ as the bifurcation parameter. It can be seen when $\tau = 0$, we have a stable endemic equilibrium (denoted by the blue curve) and unstable disease-free equilibrium (denoted by the red curve). As τ increases, the endemic equilibrium decreases. The stability types for both equilibrium do not changes, until we meet the bifurcation point BP at $\tau = 0.9172$. Passing this BP, the endemic equilibrium extinct, and the disease free equilibrium changes its stability into a stable equilibrium. A similar interpretation gives for Fig. 2(c) when we use δ as the bifurcation parameter. The BP is given at $\delta = 1.744$.

Key biological conclusion from analytical results

In this section, we have presented a detailed analysis of our model, starting with the calculation of equilibrium points, the reproduction number, and an analysis of the bifurcation diagram. These calculations are crucial in determining the long-term behavior of our TB model, particularly in assessing the impact of vaccination and treatment failure. Our analysis shows that the TB-free equilibrium is always locally asymptotically stable when the reproduction number is less than one (see [Theorem 3](#)). Furthermore, we have demonstrated that the TB-endemic equilibrium exists and is locally stable only when the reproduction number exceeds one (see [Theorem 4](#)). These results indicate that, in our proposed model, the reproduction number serves as the sole endemic indicator, determining whether TB persists or disappears. Lowering the reproduction number below one is essential to ensure the eventual eradication of TB from the population. We use a bifurcation diagram to visualize our analytical results, clearly showing that an increase in the infection rate α leads to a larger TB-endemic equilibrium. Conversely, increasing vaccine efficacy τ and the TB-induced death rate δ reduces the size of the TB-endemic equilibrium. However, the latter option is not feasible from a public health perspective.

Sensitivity analysis

The Partial Rank Correlation Coefficient (PRCC) approach is used to carry out sensitivity analyses on the parameters in the proposed tuberculosis (TB) model. This technique quantifies the sensitivity of the key model outputs, specifically the infected population and the basic reproduction number (R_0), to the individual input parameters listed in [Table 2](#), while accounting for the interdependence of other parameters. To do the analysis, we use Latin Hypercube Sampling (LHS) to produce a wide range of parameter combinations. The model is then simulated over time with these parameter sets and the PRCC values are calculated to determine how each parameter affects the result variables. Calculating the PRCC allows us to determine how each parameter affects the dynamics of the disease. [Table 1](#) describes the initial values of the compartments for the simulation: $S(0) = 10000$, $V(0) = 3000$, $L(0) = 8300$, $I(0) = 8010$, $D_r(0) = 0$, and $R(0) = 0$. LHS generates 1000 parameter sets from the provided minimum and maximum ranges, ensuring that the parameter space is sampled representatively. The PRCC technique rates the influence of each parameter based on how strongly it correlates with the output variable while accounting for the influence of other parameters. Positive PRCC values indicate a direct relationship between the parameter and the output, whilst negative PRCC values imply an inverse relationship. This research provides vital information on the parameters that most strongly control the dynamics of tuberculosis transmission and recovery, which will help guide future model development and policy interventions. The PRCC result is presented in [Fig. 3](#). The relatively low impact of vaccination aligns with the findings that the *BCG vaccine has limited efficacy in adults*, highlighting the need for more effective TB vaccines. Additionally, **TB-induced death (δ)**, **recovery (ω, ϵ)**, and **movement out of active TB** all negatively affect TB prevalence, highlighting the importance of effective treatment, drug resistance management and strengthening the health system. In general, these findings are consistent with the public health literature, emphasizing transmission reduction, early case detection, and improved treatment strategies as the most effective approaches to controlling TB. [Fig. 4](#) is the violin plot of PRCC values for the parameters of the TB model (generated distributions around the PRCC values) which visualizes the Partial Rank Correlation Coefficients (PRCC) of various parameters in the TB model, with the purpose of determining how each parameter affects the fundamental reproduction number. The position of the violin indicates the central tendency of the PRCC values, with violins centered near the top indicating a positive connection with R_0 and those placed near the bottom indicating a negative relationship. Individual points inside the violins emphasize the spread of the created synthetic PRCC values around the mean, giving a clear picture of each parameter's importance. This figure aids in identifying parameters with significant or consistent influence on the model's output, distinguishing those with a steady, predictable impact from those with greater variability or uncertainty.

Results and discussion

The results presented in this section are based on numerical simulations of the tuberculosis (TB) transmission model. In [Figs. 5](#) and [6](#), we explore the impact of transmission rates α on the dynamics of tuberculosis (TB) in different compartments. Susceptible S , vaccinated V , latent L , active I , drug-resistant D_r , and recovered R populations. We also investigated the effects of vaccination rates ϕ on the dynamics of TB in these compartments over time. These compartments depict the various phases of infection and immunity within the population. Simulating different α values allowed us to investigate how transmission dynamics affect the compartments of the TB model. These insights can be used to drive public health initiatives and inform TB epidemic management strategies. For instance, in [Fig. 6](#), the simulation shows how the vaccination rate (ϕ) influences the dynamics of tuberculosis across several compartments. The findings reveal that increasing vaccination rates dramatically reduces the number of individuals at risk, lowering the number of people who can develop latent or active tuberculosis. Higher vaccination rates also increase the vaccinated population. [Fig. 7](#) shows simulation results of TB dynamics: (a) Active TB (I) with varying γ , (b) drug-resistant TB (D_r) with varying γ , and (c) the effect of γ on the recovered population (R). [Fig. 7a](#) shows that as γ rates increase, individuals with active tuberculosis (I) recover more quickly. This means that fewer people remain in the active tuberculosis compartment over time. If treatment is highly effective (γ is high), the population in the active TB compartment will fall rapidly, potentially reaching zero by the end of the simulation time ($t = 20$). In [Fig. 7b](#), when $\gamma = 0.25$, recovery from active tuberculosis is delayed. This suggests that more patients will remain in the active TB compartment (I), with some transitioning to the drug-resistant TB compartment (D_r). Higher γ levels lead to direct recovery from drug-resistant tuberculosis, resulting in a lower D_r population. In [Fig. 7c](#), recovery from active tuberculosis is most effective when $\gamma = 1.0$. Individuals in the active TB compartment (I) migrate to the recovered (R) compartment faster than

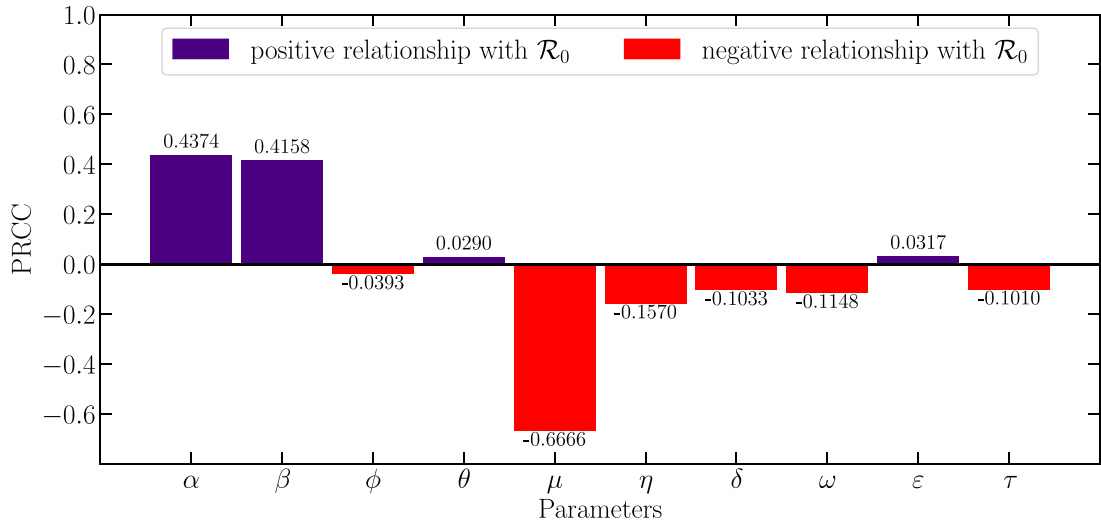


Fig. 3. PRCC result .

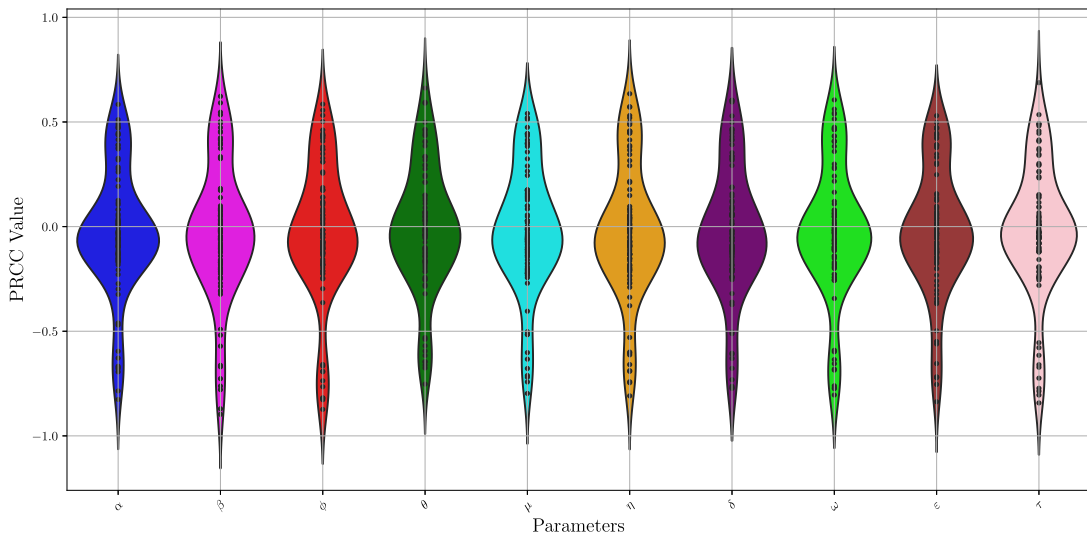


Fig. 4. Violin plot of PRCC values for TB model parameters (Generated distributions around PRCC values).

those with lower values of γ . As a result, the recovered population (R) will expand faster and attain a higher value than when γ is lower. In Fig. 8, the results show that higher recovery rates (ϵ) result in a faster reduction of drug-resistant and active TB cases, leading to a healthier and larger population. Lower recovery rates, for example, when $\epsilon = 0.1$, slow disease control leads to more infections and slower population growth. Higher recovery rates improve the effectiveness of second-line treatments in managing drug-resistant tuberculosis and promoting population recovery. Furthermore, the results show that higher values ϵ (0.4 and 0.5) result in faster recovery from drug-resistant tuberculosis and a greater increase in the recovered population (R) over time. As more people with drug-resistant tuberculosis recover, fewer people remain infected, reducing the active TB (I) and drug-resistant TB D_r populations.

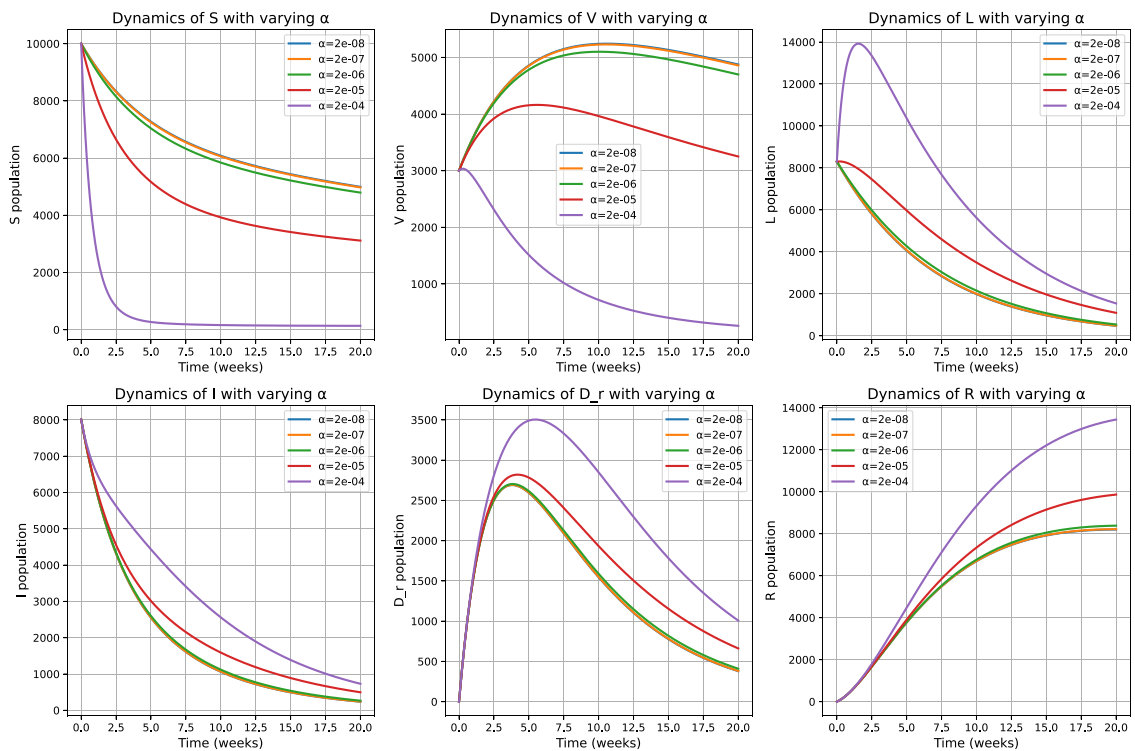


Fig. 5. Impact of Transmission Rates (α) on the Dynamics of Tuberculosis (TB) in Different Compartments: Susceptible (S), Vaccinated (V), Latent (L), Active TB (I), Drug-Resistant TB (D_r), and Recovered (R) Populations over Time.

Conclusion

Tuberculosis (TB) is an infectious disease that spreads from human to human and has been a major public health issue in many countries for years. Numerous mathematical models, each with its own specific features, have been introduced by various authors to understand the spread of TB within populations; see [24,26] for recently published studies. Unlike previous works that focus primarily on specific vaccine implementations without addressing the potential emergence of drug-resistant strains, this article presents a TB vaccination model that also considers treatment failure and the development of drug resistance. The model constructed with six compartments that account for susceptible, vaccinated, latent, active, drug resistant, and recovered populations. We established through careful mathematical analysis that in the absence of that is, the disease-free equilibrium is locally asymptotically stable when the basic reproduction number is less than unity, implying that the disease can be eradicated under certain conditions. In contrast, when the reproduction number reaches one, the endemic equilibrium exists and remains stable, highlighting the survival of tuberculosis in such settings. Our simulations offer vital information about the mechanics of tuberculosis transmission. The results show that increased vaccination rates successfully lower the susceptible population, limiting both latent and active tuberculosis cases. Increased vaccination rates also help grow the vaccinated population, illustrating the importance of vaccination programs in disease prevention. Furthermore, the study emphasizes the relevance of recovery rates in tuberculosis management. Improved recovery rates for active and drug resistant tuberculosis were found to significantly improve disease control efforts by reducing infected populations while increasing the number of recovered individuals. Finally, this study shows that effective tuberculosis control requires a combination of higher coverage of the vaccine, greater efficacy of the treatment, and lower transmission rates. These findings can help policymakers, public health practitioners, and researchers create and execute treatments to prevent tuberculosis, especially in resource-constrained areas where the illness remains a serious public health concern. Although our model already addresses the complexity of TB spread in the population by considering several important factors, such as the effects of vaccination, reinfection, treatment failure, and multidrug resistance, there are still several aspects that can be improved. The first improvement is the incorporation of incidence data to calibrate the model with real-world scenarios. Another aspect not yet included in our model is the consideration of socioeconomic characteristics, healthcare resource limitations, and the impact of diagnostic and treatment delays, which could help optimize TB control strategies. Therefore, these aspects can be explored as directions for future work.

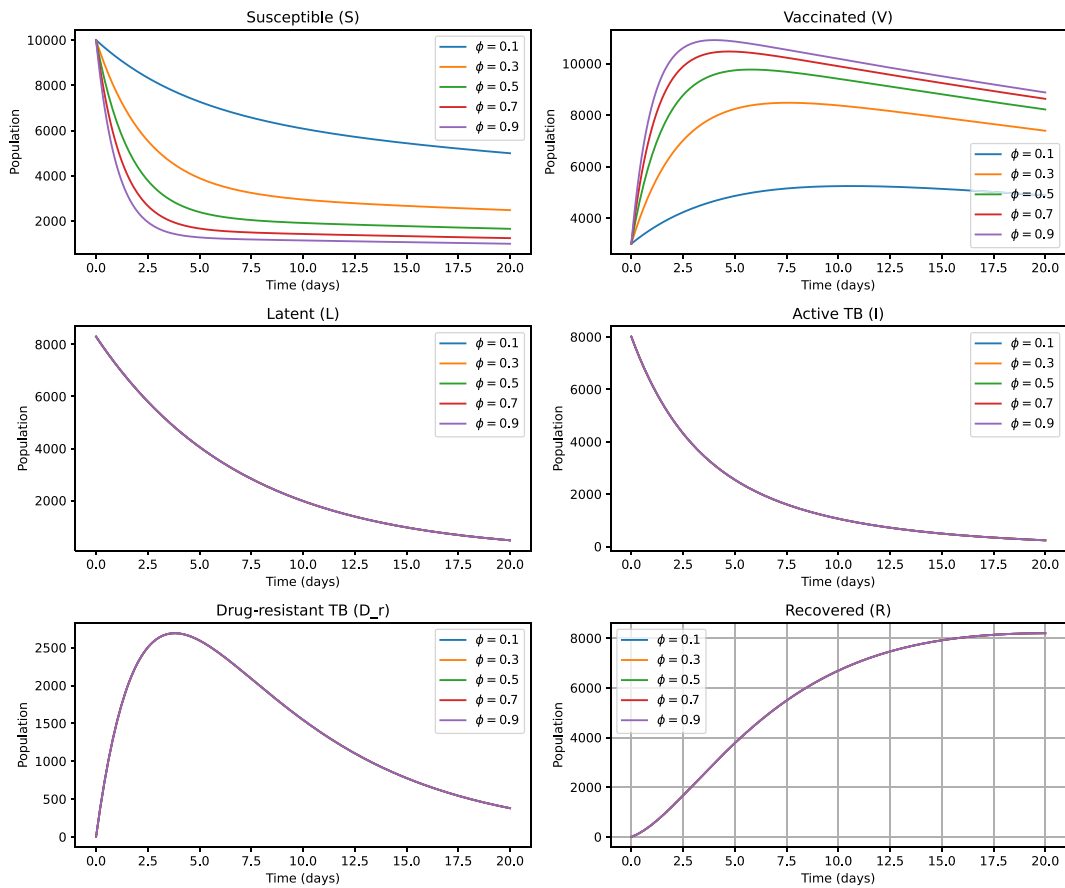


Fig. 6. Dynamic Effects of Vaccination Rates (ϕ) on TB in Different Compartments: Susceptible (S), Vaccinated (V), Latent (L), Active TB (I), Drug-Resistant TB (D_r), and Recovered (R) Populations over Time.

CRedit authorship contribution statement

Olumuyiwa James Peter: Conceptualization, Methodology, Software, Data analysis, Supervision. **Dipo Aldila:** Research design, Data collection, Data analysis. **Tawakalt Aboosedo Ayoola:** Data analysis, Interpretation, Manuscript drafting. **Ghaniyyat Bolanle Balogun:** Literature review, Manuscript writing, Critical revisions. **Festus Abiodun Oguntolu:** Data validation, Proofreading, Final manuscript editing.

Funding

DA is supported by Universitas Indonesia with PUTI Q1 research grant scheme, 2024 (ID Number: NKB-401/UN2.RST/HKP.05.00/2024).

Declaration of competing interest

The authors declare that they have no known competing financial interests or personal relationships that could have appeared to influence the work reported in this paper.

Acknowledgment

All authors reviewed and approved the final manuscript.

Data availability

Not applicable.

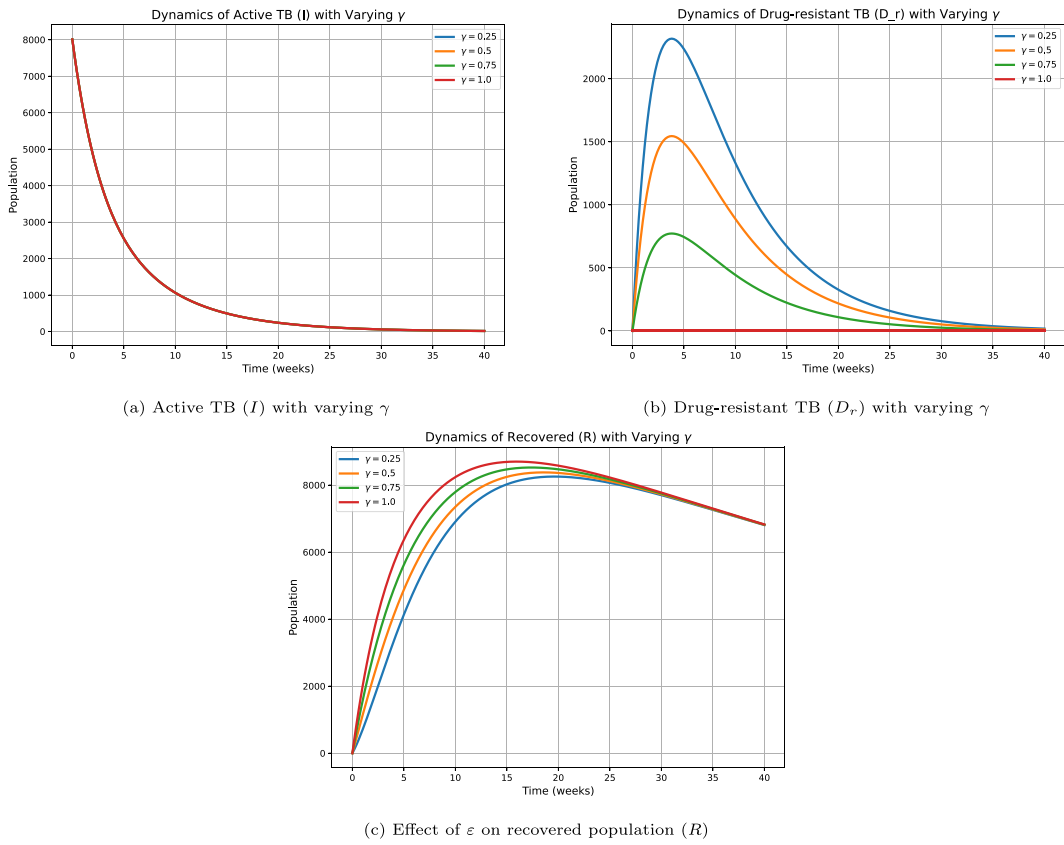


Fig. 7. Simulation results of TB dynamics: (a) Active TB (I) with varying γ , (b) Drug-resistant TB (D_r) with varying γ , and (c) Effect of γ on the recovered population (R).

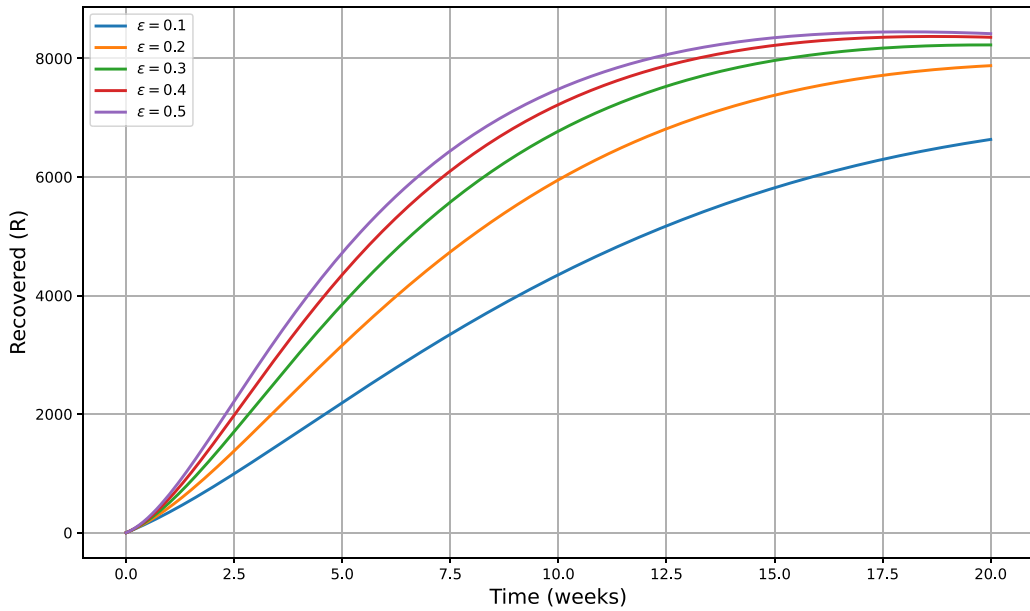


Fig. 8. Effect of recovery rate after second-line treatment.

References

- [1] N.A. Menzies, N.A. Swartwood, T. Cohen, S.M. Marks, S.A. Maloney, C. Chappelle, J.W. Miller, G.R. Beeler Asay, A.A. Date, C.R. Horsburgh, et al., The Long-Term Impacts of Domestic and International TB Service Improvements on TB Trends Within the United States: a Mathematical Modelling Study, Cold Spring Harbor Laboratory Press, 2024, MedRxiv 2024-2003.
- [2] R.C. Harris, T. Sumner, G.M. Knight, R.G. White, Systematic review of mathematical models exploring the epidemiological impact of future TB vaccines, *Hum. Vaccines & Immunother.* 12 (11) (2016) 2813–2832.
- [3] N.M. Fuller, C.F. McQuaid, M.J. Harker, C.K. Weerasuriya, T.D. McHugh, G.M. Knight, Mathematical models of drug-resistant tuberculosis lack bacterial heterogeneity: A systematic review, *PLoS Pathog.* 20 (4) (2024) e1011574.
- [4] A. Starshinova, N. Osipov, I. Dovgalyk, A. Kulpina, E. Belyaeva, D. Kudlay, COVID-19 and tuberculosis: Mathematical modeling of infection spread taking into account reduced screening, *Diagnostics* 14 (7) (2024) 698.
- [5] Y. Wu, M. Huang, X. Wang, Y. Li, L. Jiang, Y. Yuan, The prevention and control of tuberculosis: an analysis based on a tuberculosis dynamic model derived from the cases of Americans, *BMC Public Health* 20 (1) (2020) 1173.
- [6] S. Emani, K. Alves, L.C. Alves, D.A. da Silva, P.B. Oliveira, M.C. Castro, T. Cohen, R.d. Couto, M. Sanchez, N.A. Menzies, Quantifying gaps in the tuberculosis care cascade in Brazil: A mathematical model study using national program data, *Plos Med.* 21 (3) (2024) e1004361.
- [7] Y.U. Ahmad, J. Andrawus, A. Ado, Y.A. Maigoro, A. Yusuf, S. Althobaiti, U.T. Mustapha, Mathematical modeling and analysis of human-to-human monkeypox virus transmission with post-exposure vaccination, *Model. Earth Syst. Environ.* (2024) 1–21.
- [8] P.K. Rajan, M. Kuppasamy, A. Yusuf, A fractional-order modeling of human papillomavirus transmission and cervical cancer, *Model. Earth Syst. Environ.* 10 (1) (2024) 1337–1357.
- [9] B. Acay Öztürk, A. Yusuf, M. Inc, Fractional HIV infection model described by the Caputo derivative with real data, *Boletín de la Soc. Matemática Mex.* 30 (1) (2024) 1–23.
- [10] M.M. Al-Shomrani, S.S. Musa, A. Yusuf, Unfolding the transmission dynamics of monkeypox virus: an epidemiological modelling analysis, *Mathematics* 11 (5) (2023) 1121.
- [11] S. Lee, H.-Y. Park, H. Ryu, J.-W. Kwon, Age-specific mathematical model for tuberculosis transmission dynamics in South Korea, *Mathematics* 9 (8) (2021) 804.
- [12] J.M. Trauer, J.T. Denholm, E.S. McBryde, Construction of a mathematical model for tuberculosis transmission in highly endemic regions of the Asia-Pacific, *J. Theoret. Biol.* 358 (2014) 74–84.
- [13] M. Lalli, M. Hamilton, C. Pretorius, D. Pedrazzoli, R.G. White, R.M. Houben, Investigating the impact of TB case-detection strategies and the consequences of false positive diagnosis through mathematical modelling, *BMC Infect. Dis.* 18 (2018) 1–10.
- [14] A. Malek, A. Hoque, Mathematical model of tuberculosis with seasonality, detection, and treatment, *Inf. Med. Unlocked* 49 (2024) 101536.
- [15] F.O. Ochieng, Mathematical modeling of tuberculosis transmission dynamics with reinfection and optimal control, *Eng. Rep.* (2024) e13068.
- [16] H. Joshi, M. Yavuz, Transition dynamics between a novel coinfection model of fractional-order for COVID-19 and tuberculosis via a treatment mechanism, *Eur. Phys. J. Plus* 138 (5) (2023) 468.
- [17] O.J. Peter, A. Abidemi, F. Fatmawati, M.M. Ojo, F.A. Oguntolu, Optimizing tuberculosis control: a comprehensive simulation of integrated interventions using a mathematical model, *Math. Model. Numer. Simul. Appl.* 4 (3) (2024) 238–255.
- [18] M. Yavuz, M. Akman, F. Usta, N. Özdemir, Effect of the awareness parameter on a fractional-order tuberculosis model, in: *AIP Conference Proceedings*, 2483, (1) AIP Publishing, 2022.
- [19] L. Boulaasair, H. Bouzahir, M. Yavuz, Global mathematical analysis of a patchy epidemic model, *An Int. J. Optim. Control: Theor. Appl. (IJOCTA)* 14 (4) (2024) 365–377.
- [20] J. Zhang, Y. Liand, X. Zhang, Mathematical modeling of tuberculosis data of China, *Chaos Solitons Fractals* 365 (2015) 159–163.
- [21] A. Egonmwan, D. Okuonghae, Mathematical analysis of a tuberculosis model with imperfect vaccine, *Int. J. Biomath.* 13 (2019) 26–42.
- [22] S. Intan, Sriwahyuni, H. Vera, M. Syarifah, I.R. Taufiq, R. Marwan, The epidemic of Tuberculosis on vaccinated population, *J. Phys.: Conf. Ser.* 890 (2017) 012017.
- [23] E. D.A.Ginting, D. Aldila, I.H. Febiriana, A deterministic compartment model for analyzing tuberculosis dynamics considering vaccination and reinfection, *Heal. Anal.* 5 (2024) 100341, <http://dx.doi.org/10.1016/j.health.2024.100341>, URL <https://www.sciencedirect.com/science/article/pii/S2772442524000431>.
- [24] D. Aldila, J.P. Chávez, K.P. Wijaya, N.C. Ganegoda, G.M. Simorangkir, H. Tasman, E. Soewono, A tuberculosis epidemic model as a proxy for the assessment of the novel M72/AS01E vaccine, *Commun. Nonlinear Sci. Numer. Simul.* 120 (2023) 107162, <http://dx.doi.org/10.1016/j.cnsns.2023.107162>, URL <https://www.sciencedirect.com/science/article/pii/S1007570423000801>.
- [25] D. Aldila, D.A. Ramadhan, C.W. Chukwu, B.D. Handari, M. Shahzad, P.Z. Kamalia, On the role of early case detection and treatment failure in controlling tuberculosis transmission: A mathematical modeling study, *Commun. Biomath. Sci.* 7 (1) (2024) 61–86.
- [26] D. Aldila, B.L. Fardian, C.W. Chukwu, M. Hifzhudin Noor Aziz, P.Z. Kamalia, Improving tuberculosis control: assessing the value of medical masks and case detection—a multi-country study with cost-effectiveness analysis, *R. Soc. Open Sci.* 11 (6) (2024) 231715.
- [27] J. Andrawus, F. Eguda, I. Usman, S. Maiwa, I. Dibal, T. Urum, G. Anka, A mathematical model of a tuberculosis transmission dynamics incorporating first and second line treatment, *J. Appl. Sci. Environ. Manag.* 24 (5) (2020) 917–922.
- [28] K. Selain, F. Emile, H. Vinh, Analysis and simulation of a mathematical model of tuberculosis transmission in Democratic Republic of the Congo, *Adv. Differ. Equ.* 2020 (642) (2020).
- [29] S. Kim, R. Delos, E. Jung, Country-specific intervention strategies for top three TB burden countries using mathematical model, *PLoS ONE* 15 (4) (2020) 0230964.
- [30] L. Nkamba, F. Manga, M. Manyombe, Mathematical model to assess vaccination and effective contact rate impact in the spread of tuberculosis, *J. Biol. Dyn.* 13 (1) (2019) 26–42.
- [31] D. Gerberry, Practical aspects of backward bifurcation in a mathematical model for tuberculosis, *J. Theoret. Biol.* 388 (2016) 15–36.
- [32] D. Ludji, P. Sianturi, E. Nugrahani, Dynamical system of the mathematical model for tuberculosis with vaccination, *Comput. Math. Eng. Appl.* 10 (2) (2019) 59–66.
- [33] B. Mishra, J. Srivastava, Mathematical model on pulmonary and multidrug-resistant tuberculosis patients with vaccination, *J. Egyptian Math. Soc.* 22 (2) (2014) 311–316.
- [34] G. Simorangkir, D. Aldila, A. Rizka, H. Tasman, E.S. Nugraha, Mathematical model of tuberculosis considering observed treatment and vaccination interventions, *J. Interdiscip. Math.* 24 (6) (2021) 1717–1737.
- [35] F.A. Oguntolu, O.J. Peter, K. Oshinubi, T.A. Ayoola, A.O. Oladapo, M.M. Ojo, Analysis and dynamics of tuberculosis outbreak: A mathematical modelling approach, in: *Advances in Systems Science and Applications*, 2022.
- [36] K. Oshinubi, O.J. Peter, E. Addai, E. Mwizerwa, O. Babasola, I.V. Nwabufu, I. Sane, U.M. Adam, A. Adeniji, J.O. Agbaje, Mathematical modelling of tuberculosis outbreak in an East African country incorporating vaccination and treatment, *Computation* 11 (7) (2023) 143.
- [37] B.I. Omede, O.J. Peter, W. Atokolo, B. Bolaji, T.A. Ayoola, A mathematical analysis of the two-strain tuberculosis model dynamics with exogenous re-infection, *Heal. Anal.* 4 (2023) 100266.

- [38] M.M. Ojo, O.J. Peter, E.F.D. Goufo, H.S. Panigoro, F.A. Oguntolu, Mathematical model for control of tuberculosis epidemiology, *J. Appl. Math. Comput.* 69 (1) (2023) 69–87.
- [39] M.A. Khan, M. Ahmad, S. Ullah, M. Farooq, T. Gul, Modeling the transmission dynamics of tuberculosis in Khyber Pakhtunkhwa Pakistan, *Adv. Mech. Eng.* 11 (6) (2019) 1687814019854835.
- [40] S. Ullah, M.A. Khan, M. Farooq, Z. Hammouch, D. Baleanu, A Fractional Model for the Dynamics of Tuberculosis Infection Using Caputo-Fabrizio Derivative, *American Institute of Mathematical Sciences*, 2020.
- [41] S. Ullah, M.A. Khan, M. Farooq, A fractional model for the dynamics of TB virus, *Chaos Solitons Fractals* 116 (2018) 63–71.
- [42] Z. Lu, Y.H. Schukken, R.L. Smith, R.M. Mitchell, Y.T. Gröhn, Impact of imperfect *Mycobacterium avium* subsp. *paratuberculosis* vaccines in dairy herds: A mathematical modeling approach, *Prev. Vet. Med.* 108 (2) (2013) 148–158, <http://dx.doi.org/10.1016/j.prevetmed.2012.08.001>, URL <https://www.sciencedirect.com/science/article/pii/S0167587712002607>.
- [43] P.W. Ei, M.M. Htwe, M.H. Nyunt, A.S. Mon, Z. Myint, W.W. Nyunt, S.M. Win, S. Aung, W.M. Thwe, W.W. Aung, Detection of 1491F and V170F *rpoB* mutations associated with misdiagnosis of rifampicin resistance among patients with drug-susceptible tuberculosis treatment failure, Myanmar, 2022, *J. Glob. Antimicrob. Resist.* 41 (2025) 169–172, <http://dx.doi.org/10.1016/j.jgar.2024.12.026>, URL <https://www.sciencedirect.com/science/article/pii/S2213716525000013>.
- [44] T. Davenne, H. McShane, Why don't we have an effective tuberculosis vaccine yet? *Expert. Rev. Vaccines* 15 (8) (1996) 1009–1013.
- [45] N. Parrish, J. Dick, W. Bishai, Mechanisms of latency in *Mycobacterium tuberculosis*, *TIM* 6 (3) (1998) 107–112.
- [46] J.C. Palomino, A. Martin, Drug Resistance Mechanisms in *Mycobacterium tuberculosis*, *Antibiot. (Basel)* 3 (3) (2014) 317–340.
- [47] A.I. Abioye, O.J. Peter, E. Addai, F.A. Oguntolu, T.A. Ayoola, Modeling the impact of control strategies on malaria and COVID-19 coinfection: insights and implications for integrated public health interventions, *Qual. Quant.* 58 (4) (2024) 3475–3495.
- [48] O. Diekmann, J. Heesterbeek, M.G. Roberts, The construction of next-generation matrices for compartmental epidemic models, *J. R. Soc. Interface* 7 (47) (2010) 873–885.
- [49] O. Diekmann, J.A.P. Heesterbeek, J.A. Metz, On the definition and the computation of the basic reproduction ratio R_0 in models for infectious diseases in heterogeneous populations, *J. Math. Biol.* 28 (4) (1990) 365–382.
- [50] C.K. Mahadhika, D. Aldila, A deterministic transmission model for analytics-driven optimization of COVID-19 post-pandemic vaccination and quarantine strategies, *Math. Biosci. Eng.* 21 (4) (2024) 4956–4988, <http://dx.doi.org/10.3934/mbe.2024219>.
- [51] D. Aldila, J.P. Chávez, C.W. Chukwu, A.Y. Fathiyah, J.W. Puspita, K.A.D. Setio, A. Fuady, P.Z. Kamalia, Unraveling dengue dynamics with data calibration from Palu and Jakarta: Optimizing active surveillance and fogging interventions, *Chaos Solitons Fractals* 189 (2024) 115729, <http://dx.doi.org/10.1016/j.chaos.2024.115729>, URL <https://www.sciencedirect.com/science/article/pii/S0960077924012815>.
- [52] I.H. Febiriana, A.H. Hassan, D. Aldila, Enhancing malaria control strategy: Optimal control and cost-effectiveness analysis on the impact of vector bias on the efficacy of mosquito repellent and hospitalization, *J. Appl. Math.* 2024 (1) (2024) 9943698.
- [53] H. Tasman, D. Aldila, P.A. Dumbela, M.Z. Ndi, Fatmawati, F.F. Herdicho, C.W. Chukwu, Assessing the impact of relapse, reinfection and recrudescence on malaria eradication policy: a bifurcation and optimal control analysis, *Trop. Med. Infect. Dis.* 7 (10) (2022) 263.
- [54] C. Castillo-Chavez, B. Song, Dynamical models of tuberculosis and their applications, *Math. Biosci. Eng.* 1 (2) (2004) 361.
- [55] M.A. Kuddus, E.S. McBryde, A.I. Adekunle, L.J. White, M.T. Meehan, Mathematical analysis of a two-strain tuberculosis model in Bangladesh, *Sci. Rep.* 12 (1) (2022) 3634.
- [56] I.M. Wangari, S. Davis, L. Stone, Backward bifurcation in epidemic models: Problems arising with aggregated bifurcation parameters, *Appl. Math. Model.* 40 (2) (2016) 1669–1675.
- [57] A. Egonmwan, D. Okuonghae, Mathematical analysis of a tuberculosis model with imperfect vaccine, *Int. J. Biomath.* 12 (07) (2019) 1950073.
- [58] M.A. Kuddus, M.T. Meehan, L.J. White, E.S. McBryde, A.I. Adekunle, Modeling drug-resistant tuberculosis amplification rates and intervention strategies in Bangladesh, *PLoS ONE* 15 (7) (2020) e0236112.
- [59] Y. Yang, J. Li, Z. Ma, L. Liu, Global stability of two models with incomplete treatment for tuberculosis, *Chaos Solitons Fractals* 43 (1–12) (2010) 79–85.
- [60] F. Sulayman, F.A. Abdullah, M.H. Mohd, An SVEIRE model of tuberculosis to assess the effect of an imperfect vaccine and other exogenous factors, *Mathematics* 9 (4) (2021) 327.